Study of effective removal of nickel and cobalt from aqueous solutions by FeO@mSiO2 nanocomposite

Wahran M. Saod [a,*], Nisreen Jassam Alaallah [b], Ekhlas A. Abdulkareem [c], Nahla Naji Hilal [d], Mohammad I. AlBiajawi [e]

[a] *Department of Chemistry, College of Science, University of Anbar, Ramadi, Iraq*
[b] *Department of Chemistry, Directorate of Education Anbar, Ministry of Education, Iraq*
[c] *Department of Chemistry, College of Science, University of Diyala, Iraq*
[d] *University of Fallujah, Scientific Affairs Department, Fallujah, Iraq*
[e] *Faculty of Civil Engineering Technology, Universiti Malaysia Pahang AL-Sultan Abdullah, Persiaran Tun Khalil Yaakob, 26300 Gambang, Pahang, Malaysia*

ARTICLE INFO

ABSTRACT

In many regions of the world, water pollution from potentially harmful substances like nickel (II) and cobalt (II) ions is a recurring issue. The quality of rivers and lakes' environments, wastewater discharge, and drinking water sources are all still significantly impacted by it. Many studies are focused on developing new treatment alternatives since, although treatment is often necessary, it is not always possible or accessible in a particular setting. Nanotechnology provides significant potential for water treatment. Although it has been demonstrated that nanomaterials may effectively remove both different type from chemical pollutants—including organic and inorganic—from contaminated source, their removal efficacy may be diminished by their propensity to flocculate. Iron oxide loaded with mesoporous silica (FeO@mSiO$_2$) was effectively synthesized and characterized through the use of FTIR, SEM, TGA, XRD, and UV–visible spectral analysis. Tests and evaluations were conducted to determine FeO@mSiO$_2$ nanocomposite ability to remove nickel (II) and cobalt (II) from solution, and the ideal removal conditions were determined at different condition Adsorption isotherms, Freundlich and Temkin isotherms to the data. FeO@mSiO$_2$ composite material displayed significant efficacy in the removal of Ni and Co. The best removal rates were attained at pH 7 and 180-minute contact duration.

Introduction

Nickel and cobalt ions are among the list of toxic heavy metal ions that pose a major threat to the aquatic environment, as they are not biodegradable. in sewage and wastewater. They have been classified as toxic pollutants and as substances of priority according to the Clean Water Act of several international organization for water. Consequently, these metals are considered to be among the most dangerous pollutants typically found in water [1,2]. The main sources of water contamination with nickel and cobalt ions include electroplating, battery manufacturing, smelting, mining, refining, and printing processes, metal finishing, and other processes contribute to the release of these toxic metals into the water. /Furthermore, increased levels of nickel and cobalt in the environment have resulted in several health hazards, including Skin conditions, nausea, persistent asthma, coughing, low blood pressure, lung irritation, paralysis, diarrhea, and bone

deformities, as well as genetic alterations in living cells [3,4]. Therefore, it was necessary to search for techniques to treat water contamination with metal ions. Different techniques include oxidation- reduction, membrane filtration [5], coagulation [6], chemical precipitation [7], solvent extraction, flocculation [8], electrochemical treatment, ion exchange [9], reverse osmosis [10], evaporation, precipitation [11], and black sand filtration assisted by UV light [12]. These technologies can be good option in reduce water contamination, but they are expensive, the high cost of this techniques makes its application less economically attractive in industrial scale, complex operations, require high energy, and lead to the generation of by-products that require additional technologies to get rid of them. Therefore, adsorption is a promising technique found to be quite suitable, cheap, and more effective for removing Ni(II) and Co(II) from contaminated water [13]. During adsorption, substances typically transfer from the different phases (liquid or gas) to the solid cover and interact through physical forces, ion exchange, or

* Corresponding author.
E-mail address: sc.wahran.s@uoanbar.edu.iq (W.M. Saod).

chemical bonds [14]. The adsorbent can also be renewed by an appropriate desorption process, as the adsorption process is sometimes reversible. Additionally, the adsorption method is excellent for removing metal ions from contaminated solutions when their concentration is low [15]. Different adsorbents, such as agricultural wastes, natural substances, Sugar beet crown (SBC) [16], seaweeds, crab shell, and waste factory tea, chelating minerals, biopolymers, and activated carbon [14]. activated carbon which is one of the most crucial/best techniques for removing heavy ions metal from waste water. Due to high effective surface area, activated carbon has many benefits which is related to its high volume of micropores and mesopores [17]. This technique has been employed by numerous researchers to remove organic and inorganic from polluted water.Activated carbon has many benefits such as low cost and its muiltiple sources [18,19]. Addition, many of studied was using mesopuoros silica and ananocomposite to removal heavy metals. All those metals improve effectiveness in removal [2,20,21].

Therefore, it was necessary to develop new adsorbents with higher removal efficiency. Therefore, one of the most promising technologies for the exclusion of Ni and Co ions from water solution is nanotechnology [22,23]. The nanoparticles' unique physical and chemical characteristics at the nanoscale have been observed [24]. Several metal oxide nanoparticles have shown potential as nano adsorbents for environmental remediation. These include alumina (Al_2O_3) [25], zinc oxide (ZnO) [26], titanium dioxide (TiO_2) [27], and iron oxide nanoparticles (FeO@mSiO$_2$ nanocomposite) [28,29]. Among the nanoparticles above, the FeO@mSiO$_2$ nanocomposite has demonstrated considerable potential as a nano adsorbent for environmental remediation. This phenomenon can be attributed to the significant ratio between their surface area and volume and their elevated surface energies [30]. In addition, it is worth noting that these iron oxide nanoparticles (IONPs) possess the advantageous characteristics of recyclability and low cost [31]. Nevertheless, the efficacy of metal nanoparticles as sorbents may be compromised when used independently due to aggregation and associate phenomena in the context of water treatment [32]. Therefore, it was necessary to find a way to improve the properties of this material.

In this study, we are embedding iron oxide nanoparticles (FeO@mSiO$_2$ nanocomposite) with silica in stable matrices that have unique properties for increasing the efficiency of removal heavy metals from water.

The synthesis has a lower level of complexity compared to composite materials, which makes the synthetic technique simpler, more repeatable, and easier to scale-up].,Ensuring the capacity of a substance to be broken down by natural processes, and the prevention of using substances that are harmful or not authorized [33,34,35,36,37,38,39]. The toughness and durability of oxide nanoparticles, especially when compared to organic or polymeric nanoparticles, is noteworthy. Also, Iron oxide particles exhibit a far lower sensitivity to variations in size or shape dispersion compared to other heat mediators, especially plasmonic nanoparticles, in terms of their photothermal performance [40,41,42]. Many of studied was using mesopuoros silica,ananocomposite and activated carbon to removal nickel and cobalt. All those metals improve effectiveness in removal [43 20]. Current studies have used a different absorbent materials form remove nickel and cobalt from wastewater [44,45,46,47].

The present study focus to synthesis FeO@mSiO$_2$ nanocomposite, the generated FeO@mSiO$_2$ nanocomposite have been tested for their capacity to strip off Ni (II) and Co (II) from aqueous solutions in direct. Optimal conditions (pH, adsorbent to solution ratio, and equilibration time) for heavy metals removal have been also determined.

Experimental

Materials

All reagents used in the preparation were of high purity: Iron oxide nanoparticles, tetraethyl orthosilicate,and cetyltrimethyl bromide were purchased from Sigma-Aldrich, UK.Ammonium chloride from ACROS, nickel nitrate and cobalt nitrate tetrahydrate; from BDH, UK.

Synthesis of FeO@mSiO$_2$ nanocomposite

Nanocomposite was synthesized ensuing elsewhere an approach reported. 0.10 g of Fe NPs,60 ml of C_2H_5OH and 1.2 ml of (NH4OH; 28 wt %) were mixed under ultrasonic for 1 h. 0.30 g of CTAB was added to the mixture, followed by dropwise addition of 0.43 ml of TEOS with stirring. The mixture was stirred at 25 °C for 6 h. The mixture was separated and washed with HCl and deionized water, Then it was dried at 100 °C for overnight and calcined at 500 °C for 3 h [48,49].

Metal adsorption studies

Stock solutions containing nickel (II) and cobalt (II) ions at a concentration of 1000 mg/L were generated by dissolving appropriate quantities of Ni $(NO_3)_2$·$6H_2O$ and $Co(NO_3)$·$6H_2O$. The salts were dissolved in deionized water and diluted to provide standard solutions with concentrations ranging from 10 to 100 mg/L of Ni(II) and Co(II). The pH of the solution was changed either hydrochloric acid (1M HCl) and (1M NaOH) solutions. All chemicals and reagents utilized in the experiment were procured in analytical purity, employed without any purification procedures, and obtained from Sigma-Aldrich.

Characterization of FeO@mSiO$_2$ nanocomposite

The FeO@mSiO2 nanocomposite was studied utilizing UV–Vis spectrophotometry (UV-Cary 60, Agilent) and Fourier-transform infrared spectroscopy (Bruker). Moreover, Powder X-ray diffraction (XRD) patterns were obtained using a Bruker D8 Advance apparatus diffractometer,. Thermogravimetric analysis (TGA) was examined utilizing STA 1500 apparatus. The morphology materials was examined utilizing field emission scanning electron microscopy (S-4500, HITACHI).

Batch adsorption studies

The capacity of FeO@mSiO$_2$ nanocomposite to strip off Ni and Co ions from its solutions was considered utilizing adsorption batch tests in a shaking shaker. The ideal adsorption conditions should be determined, these experiments looked at the prepared FeO@mSiO2 nanocomposite susceptibility to removing nickel and cobalt ions from aqueous solutions under several conditions, such as pH ranging from 3 to 9, contact time ranging from 15 to 180 min, initial concentrations of nickel and cobalt (10 to 100 mg/L), and adsorbent dose on nickel and cobalt adsorption efficiency (10 to 80 mg in 25 ml). In each experiment, 100 mg/L of FeO@mSiO2 nanocomposite was combined with 25 ml of solutions containing various amounts of cobalt and nickel ions. In each experiment, 100 mg of FeO@mSiO$_2$ nanocomposite was combined with 25 ml of solutions containing various amounts of cobalt and nickel ions. The samples were centrifuged at 5,000 rpm for 10 min to remove any remaining suspended material after being shaken in a water bath at 100 rpm to make sure the adsorbent and adsorbate made great contact with one another. A final atomic absorption device was used to calculate the sample's nickel and cobalt concentrations. At room temperature all experiments carried out. The percentages of the removal efficiency (%R) and the adsorption capacity (qe) for nickel and cobalt ions, respectively, were calculated using Eqs. (1) and (2).

$$\%R = \frac{(Co - Ce)}{Co} \times 100 \tag{1}$$
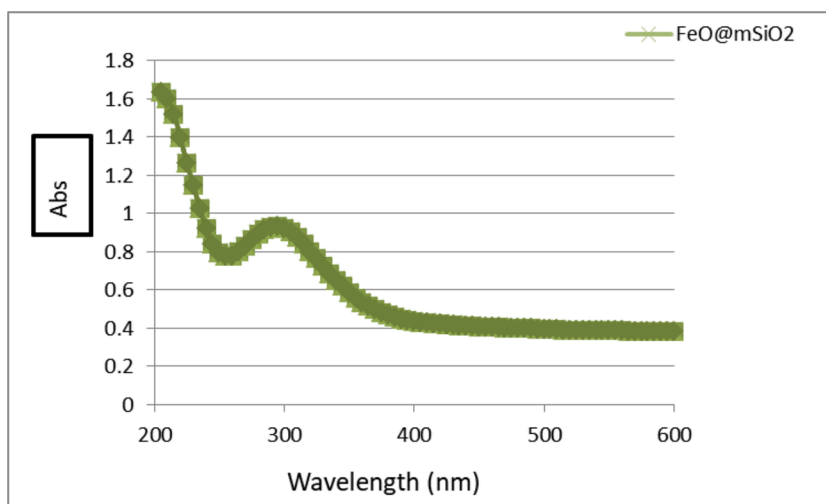
$$qe = \frac{(Co - Ce) \times V}{m} \tag{2}$$

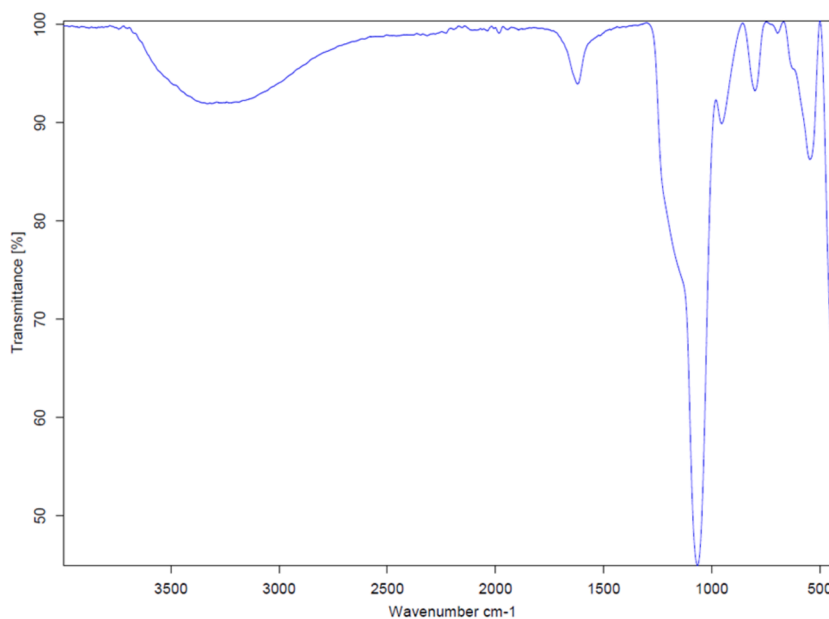**Fig. 1.** Uv–Vis for FeO@mSiO$_2$ nanocomposite.

Page 1 of 1

Fig. 2. FTIR spectra of for FeO@mSiO$_2$ nanocomposite.

where,

Co: represent the initial metals ion concentrations (mg/L).
Ce: the concentration of metals ion at equilibrium (mg/L).
M: the mass of synthesis adsorbent (g), and V: volume of solution (l).

Result and discussion

Characterization of FeO@mSiO$_2$ nanocomposite

Uv–visible spectroscopy

Fig. 1 displays the UV–vis spectra of FeO@mSiO$_2$ nanocomposite. We conducted UV–Vis spectroscopy to observe the substance has a peak at 300 nm, which is distinguish for iron oxide.

Fourier transforms infrared spectroscopy

FTIR spectra of studied materials FeO@mSiO$_2$ nanocomposite @mSiO$_2$ are presented in Fig. 2.FeO@mSiO$_2$ nanocomposite −mSiO$_2$, a broad band at ~3419 cm^{-1} due to the O-H and N–H bond stretching vibrations. The band at 1634–955 cm^{-1} may be indicative of C=O and C=C stretching. While the band at 755 cm^{-1} may be indicative of carbonate species bound to metal oxide surface.

X-ray diffraction

Crystalline properties of FeO@mSiO$_2$ nanocomposite was evaluated from the XRD patterns as Fig. 3. Characteristic peaks were observed at 24°, 30°, 33°, 36°, 39°, 41°, 43°, 49°, 54°, 57°, 63° and 65° for FeO@mSiO$_2$ nanocomposite nanoparticles, corresponding to (111) crystal plane, (220), (311), (222), (400), (422), (511), (440), (620), (533) and (622) can be indexed into cubic structures. The XRD pattern of FeO@mSiO$_2$ nanocomposite shows weak and broad peaks between 24° and 33°, which is attributed to the amorphous structure of the SiO$_2$ shell. In addition, the strong and sharp peaks at 33° and 36° indicate the crystalline nature.
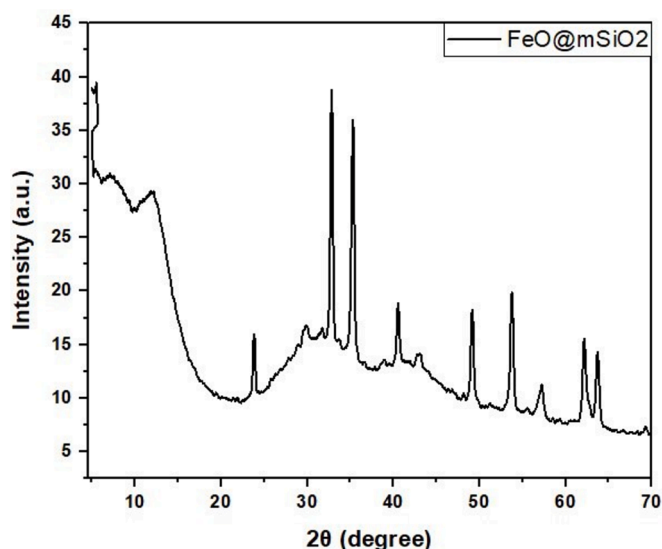
Fig. 3. XRD spectra of FeO@mSiO2 nanocomposite @mSiO2.

Scanning electron microscopy

FeO@mSiO2 nanocomposite surface morphology was studied using SEM Fig. 4. According to the XRD data for this material, the FeO@mSiO2 nanocomposite showed a morphology that approximated highly organized crystal flakes or shards. For this sample, an average iron to silica atomic ratio of 4 is determined by the SEM-EDX analysis Fig. 5.

Thermal analysis

The TG-DTA properties for FeO@mSiO$_2$ nanocomposite as show Fig. 6. The first mass loss from material below 100–160 °C is an indication the of water removal that is present as physisorbed H$_2$O on FeO@mSiO$_2$ nanocomposite. The second weight loss from 300 to 400 oC is attributed to the formation of intermediate hematite (α-Fe$_2$O$_3$) phase. Between 400 and 800C, the sample's weight is unaffected, and no weight loss is seen.

Adsorption studied

Effect of pH

The acid and basic level of the solution is a significant factor in eliminating Co (II) and Ni (II) ions from an aqueous solution using FeO@mSiO$_2$ nanocomposite. The pH of the solution influences both the dissociation of functional groups and the chemical properties of the solution, significantly affecting its adsorption. Capabilities [49–51]. In this part of experiment, the effect of changing the pH scale of the solution on the removal of Ni (II) and Co (II), were investigated by adjusting the pH of the solution from 3 to 9 with initial concentration of 100 mg/L. The contact time was set at 3 h, and the quantity of adsorbent used was 0.1g. According to the depiction in Fig. 7, the adsorption of ions on the
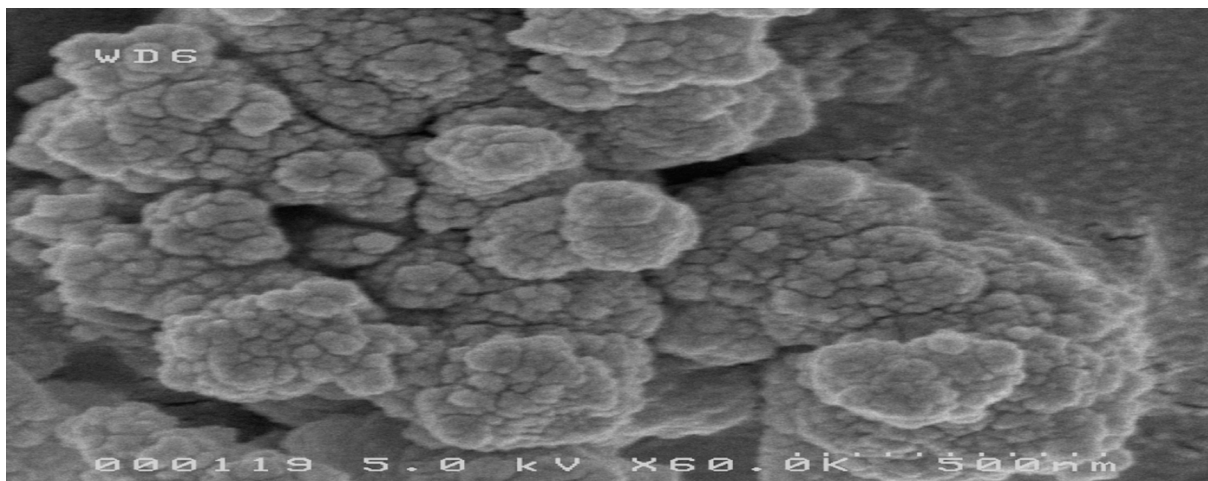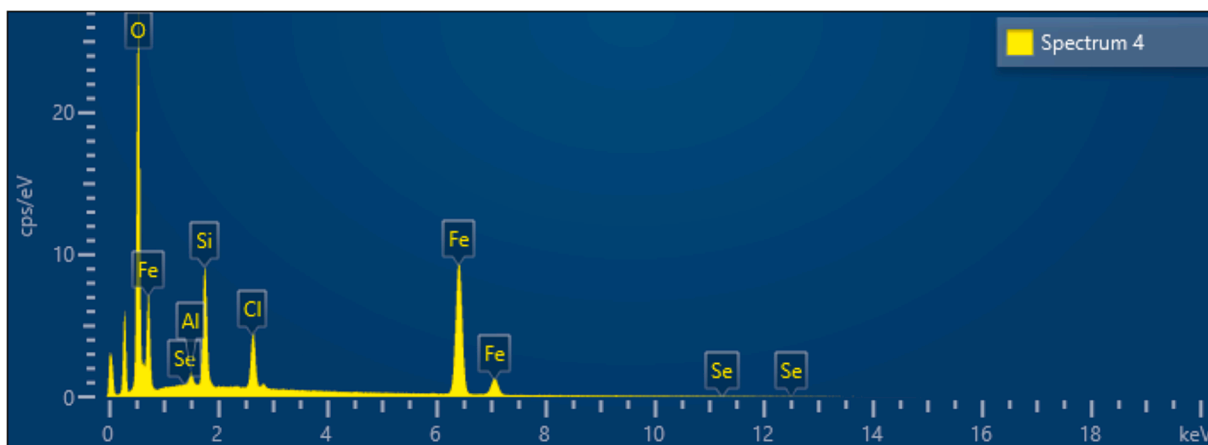

Fig. 4. SEM images for FeO@mSiO$_2$ (500 nm).

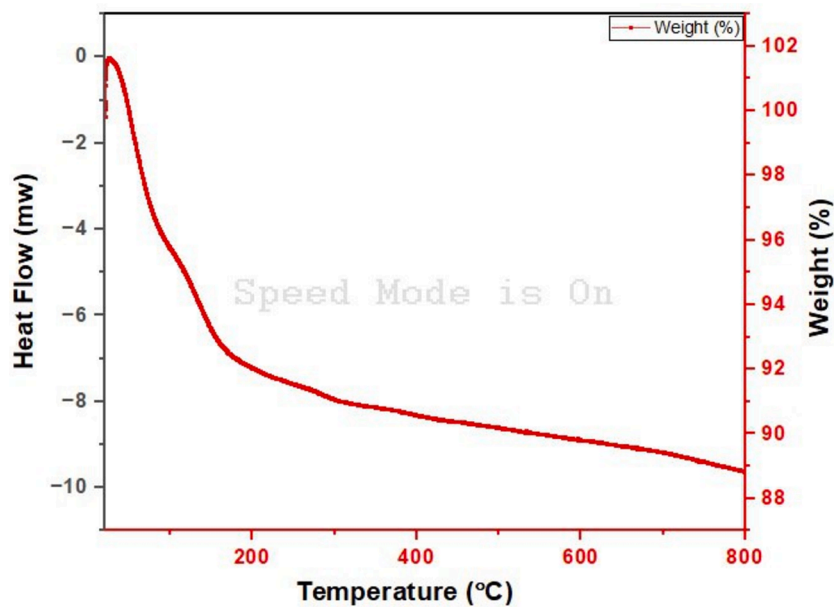**Fig. 5.** EDS of FeO@mSiO$_2$ nanocomposite.

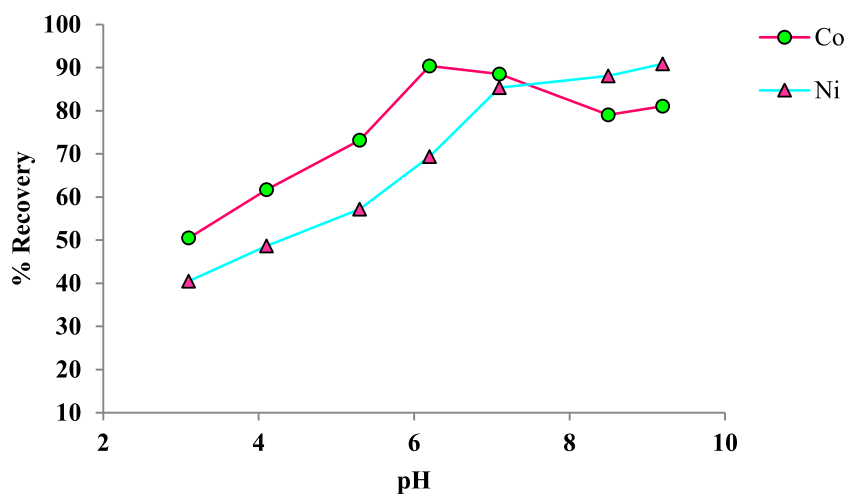**Fig. 6.** TGA data for FeO@mSiO$_2$ nanocomposite.

Fig. 7. Effect of pH on % Ni(II) and Co(II) removal, with an initial solution concentration of 100 mg/L, 25 mg of adsorbent, a solution volume of 25 mL, and an equilibrium time of 3 h.
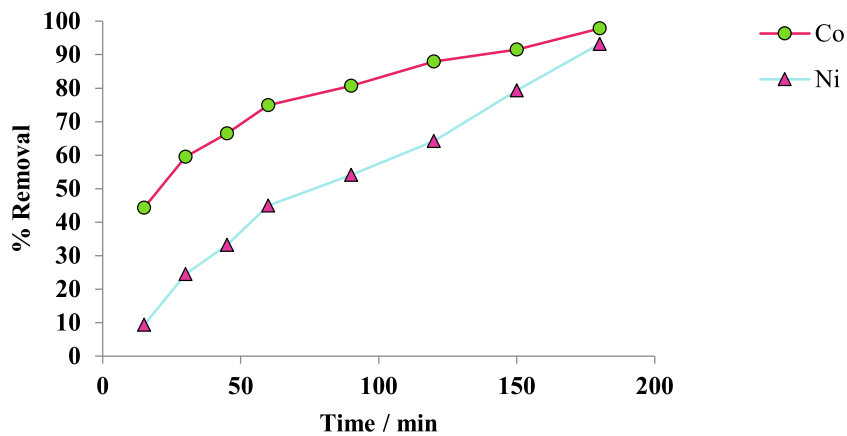

Fig. 8. Effect of contact time on % Ni(II) and Co(II) removal at pH 6.5, initial concentration 100 mg/L, 25 mg adsorbent, and 25 mL total volume.
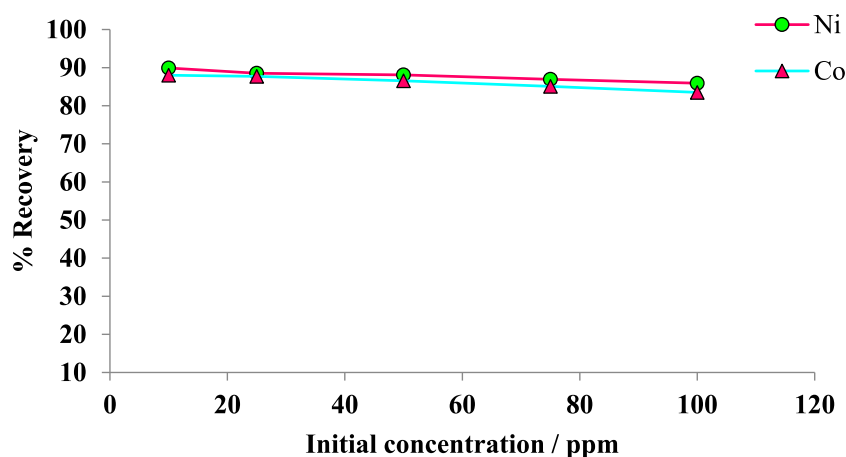
Fig. 9. Effect of initial concentration on % Ni(II) and Co(II) removal by the adsorbents with conditions set at pH 7, temperature 25 °C and sorbent dose 25 mg: 25 ml solution.
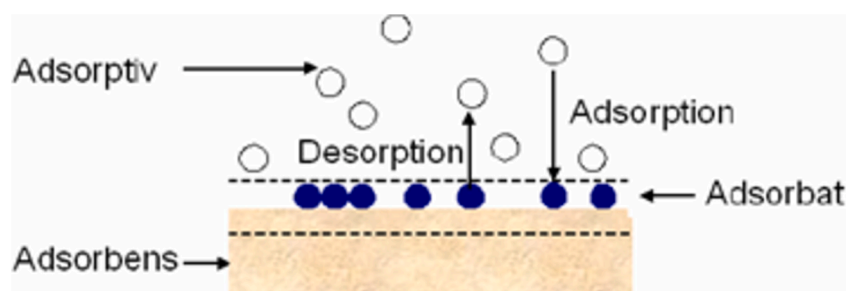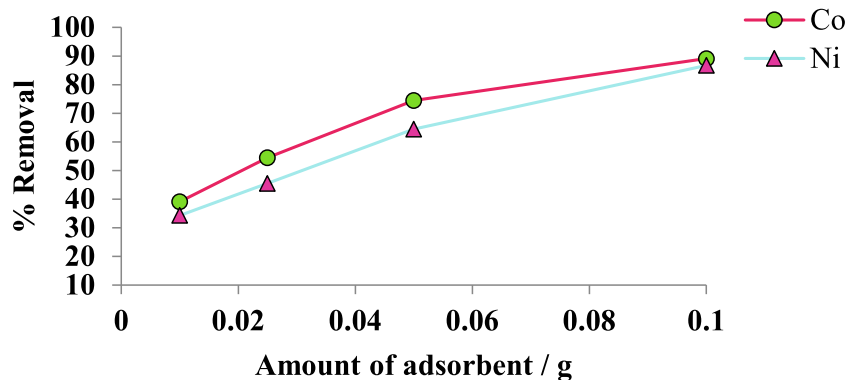

Fig. 10. Adsorption process [61].

Fig. 11. Effect of adsorbent dose on % Ni(II) and Co(II) removal with conditions set at pH 6.5, temperature 25 °C, total volume 25 ml, and initial concentration 100 mg/L.

$FeO@mSiO_2$ nanocomposite at room temperature was shown to be considerably adopted by the pH of the solution.

The results can be divided into two pH regions. The first pH region is from 3 to 5, in which the removal efficiency of nickel and cobalt significantly rises when the pH level increases. As an illustration, the removal efficiency of Ni (II) exhibited a notable enhancement from 5% to 85%, but the removal efficiency of cobalt saw an increase from 10% to 80% as the pH level was elevated from 3 to 5. The relationship can be described in terms of the charge of the adsorptive surface and the concentration of hydrogen ions in the solution. To clarify, when the pH level falls below three (pH < 3), the con of (H^+) in the surrounding medium is elevated. Hence, the adsorbent's surface exhibits a non negative charge. Competition between metal ions and H+ ions and repulsion between metal ions and positively charged adsorbent particles were observed [4].

The binding sites on the protons on the surface of the adsorbed material are no longer available, thus affecting its ability to bind to cationic metals [51]. In the second pH region, from 5 to 9, optimum removal was achieved. For nickel, it was approximately 93% at pH 8.6, after which it began to decline, while the optimal removal of cobalt was approximately 97% at pH 6, after which the removal efficiency remained almost constant. Perhaps this can be explained by with the pH increase of the solution, more negatively charged on the surface of $FeO@mSiO_2$ nanocomposite can be available for the ion-exchange of Ni^{2+}. This enhanced negative charge facilitates the ion exchange process of Ni^{2+}, leading to an augmentation of the adsorption capacity for Ni^{2+}. Upon the increase in pH, the adsorption capacity tended to stabilize, ultimately reaching a plateau and ceasing any further increase. However, the observed decrease in adsorption capacity can be attributed to the rise in OH^- ions

Table 1

Parameters and equations of the Freundlich,Langmuir and Temkin linear isotherm model.

Freundlich	Line equation	R^2	1/n	KF
Ni_FeO@mSiO2	y = 0.86015x + 0.8987	$R^2 = 0.9964$	0.8615	7.919
Co_FeO@mSiO2	y = 0.865x + 0.9539	$R^2 = 0.999$	0.7493	7.328
Langmuir	Line equation	R^2	qm, (mg/g)	KL (L/mg)
Ni_FeO@mSiO2	y = 0.1317x + 0.0036	$R^2 = 0.999$	277.8	0.00047
Co_FeO@mSiO2	y = 0.01081x + 0.0049	$R^2 = 0.9987$	204	0.000662
Temkin	Line equation	R^2	BT (J/mol)	KL (L/mg)
Ni_FeO@mSiO2	y = 24.235x + 0.3504	$R^2 = 0.9526$	24.235	1.01
Co_FeO@mSiO2	y = 28.616x + 0.7475	$R^2 = 0.9255$	28.616	1.026

Table 2

The pseudo-second-order kinetic for Ni(II) and Co(II) ions.

FeO@mSiO$_2$	Model	Constant	Value
Ni	Pseudo-2nd-order Kinetic parameters	$q_{e(exp)(mg/g)}$ (mg/g)	2.786
		K_2 (g mg^{-1} min^{-1})	136.99
		R^2	0.964
Co	Pseudo-2nd −order Kinetic parameters	$q_{e(exp)(mg/g)}$ (mg/g)	4.87
		K_2 (g mg^{-1} min^{-1})	0.256
		R^2	0.9989

within the solution's environment. This increase leads to metal hydroxide precipitates and soluble hydroxylated complexes of the metal ions. These species compete with the active sites on the FeO@mSiO$_2$ nanocomposite, resulting in no significant increase in adsorption capacity [52,53]. It is important to observe that as the pH of the stock solution was elevated beyond pH 9, there was a drop in the percentage removal of nickel.

Therefore, the adsorption mechanism changes due to the high concentration of negatively charged species on the surface. This results in attraction electrostatic between negatively charged species and cationic metal ions, resulting in increased binding of cationic metal ions [54]. Previous studies have demonstrated similar principles for the adsorption of various metal ions by biosorbents [49,55].

Effect of contact time

Another parameter that effectively affects the deletion of Ni (II) and Co (II) from its solutions is the contact time. Therefore, it is important to optimize the contact time in order to achieve maximum absorption efficiency. The connection time at which the metal adsorption rate reaches its maximum efficiency is imperative. The pH values of 6.5 that were previously tuned for nickel and cobalt ions [2]. The highest removal efficiency of nickel and cobalt was recorded after 3 h approximately was 95%, for nickel and 98% for cobalt as Fig. 8.

This can be explained by the increase in contact time leading to an increase in the chances of collision between the particles of the adsorbent surface and the heavy ions of the contaminant to be removed [4]. The result obtained in this study is excellent agreement with another study [56–58].

Effect of concentration. Single of the most important factors in the adsorption of Ni (II) and Co (II) by FeO@mSiO2 nanocomposite as adsorbent material is the ratio of its quantity to concentration of the heavy metals. Batch-wise adsorption experiments were conducted on the treated FeO@mSiO$_2$ nanocomposite to determine the most effective adsorbent. The objective was to explore the adsorption of Ni (II) and Co (II) ions under specific conditions performed at 25°C, pH 6.5, the adsorbent 10 m., with range of concentration of Ni (II) and Co (II) ions from 10 mg/L to 100 mg/L. The percentage of nickel and cobalt adsorption on FeO@mSiO2 nanocomposite −mSiO2 concerning the adsorbent is shown in Fig. 9.

Results of this investigation indicate that adsorption effectiveness is directly related to the surface area of the adsorbent (the amount of adsorbent in solution). This phenomenon is explained by the increase in surface area, which provides more active sites for the binding of metal ions. As a result, this results in an increased removal rate of heavy metal ions from polluted water [49]. The results of this study align with those found in previous literature [58,59].

The mechanism by which biochar removes heavy metal pollutants involves the physical adsorption(SSA) process, specifically through the interaction of carboxyl (R-COOH) and hydroxyl (O–H) groups Fig. 10. This process effectively removes pollutants such as Cu(II), Ni(II), Pb(II), Zn(II), Cd(II), and Hg(II). Additionally, Cr(VI) is reduced to Cr(III) as the oxygen-containing functional group adsorbs Cr(III) and Al(III) at lower pH levels [60]. Our finding of this study is consistent with other studies [61].

Dose of adsorbed. The ions of metal dosage absorbed from the aqueous medium depends on the range of concentration of ions in the polluted solution. Experimental studies are necessary to determine the most
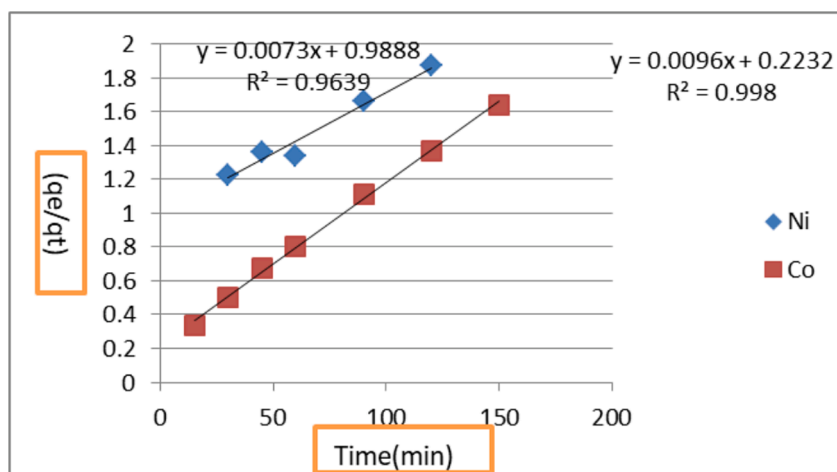

Fig. 12. The pseudo-second-order kinetic for Ni (II) and Co (II) ions.

favorable concentration of metal ion solutions while keeping other parameters constant., temperature 25°C, pH 8–9, initial concentrations of Ni and Co ions (100) mg/L, and different amount of adsorbent $FeO@mSiO_2$ nanocomposite (10, 30, 50, and 100) mg, Fig. 11 shows the results obtained in this experiment. The results show that when the dose is 10 mg/L, the removal efficiency of nickel and cobalt is about 99% [62,63].

At a concentration of 100 mg/L, the removal efficiency was 95% for nickel and 97% for cobalt. The results indicate that the adsorption efficiency reduced with growing concentration of polluting ions. This can be explained by the decrease in the number of active sites available on the surface of the adsorbent material to bind to heavy metal ions in the polluted solution [19,63].

Sorption isotherms

In order to explain the covering process on the surface of a solid adsorbent, which is characterized by homogeneity and depends on the action of the material being adsorbed at constant temperature, Langmuir presented an isothermal model [64]. It is assumed that the active site responsible for adsorption can form covalent, ionic, or coordination bonds, with minimal interaction between the adsorbed molecules. In order to obtain the maximum adsorption capacity, the particles being adsorbed organize themselves into a monolayer on the adsorbent's surface, which is where adsorption particularly occurs [2,65,66]. Linearized Freundlich, Langmuir and Temkin adsorption isotherms for Ni(II) and Co(II) are shown in the Table 1.

The distribution coefficient and differences from linearity are indicated by the Freundlich model isotherm parameters KF and 1/n, respectively. The latter can also be viewed as a measure of adsorption intensity. The affinity and heterogeneity of the adsorbent sites increase with decreasing 1/n value. The qm values for Ni (II) and Co (II) adsorption on FeO@mSiO2 are 277.8 mg/g, 204 mg/g, and 80.6 mg/g, respectively. While 1\n in Freundlich model in (0.8615,0.7493)in orderly. 0 < nf < 1, where nf > 1 indicates unfavorable adsorption and nf = 1 indicates linear adsorption. When nf = 0, the adsorption process is irreversible [67]. Langmuir and Freundlich models fitted best ($R^2 >$ 0.996) and indicated that the major contribution to Ni (II) and Co (II) removal process is via adsorption rather than a catalytic reaction. The results of the Temkin model are also same with other models, with Ni(II) being more affected by adsorption affinity than Co(II), as shown in Table 1.

Adsorption kinetics

Adsorption kinetics examines the relationship between reactants and contact duration. Kinetic models are essential for analyzing the adsorption process involved in the removal of hazardous heavy metals [68,68]. The two predominant kinetic theories are pseudo-first order and pseudo-second order kinetics [69,70].

The first and second pseudo order models

Pseudo-first-order, pseudo-second-order, and intraparticle diffusion kinetic models were applied [70]. The linear form of the pseudo-first-order kinetic model is expressed as Equation (1.1)

$$\ln(q_e - q_t) = \ln q_e - k_1.t \qquad (1.1)$$

where q_t is the amount of adsorbed ion per gram of adsorbent at time t, and k1 is the constant adsorption rate of the pseudo-first-order kinetic model.

The linear form of the pseudo-second-order kinetic model is given by Equation (1–2):

$$\frac{t}{q_t} = \frac{1}{k_2 \times q_e^2} + \frac{t}{q_e}$$

where K_2 is the constant of the pseudo-second-order kinetic model

By studying the matching between the calculated and it was confirmed that (qe (cal.) = 2.786 and 4.87 mg/g, as shown as Table 2.

As well, Fig. 12 obtained from the pseudo-second-order kinetic model were higher than that obtained from the pseudo-first-order kinetic model Ni(II) and Co(II) ions indicating that the pseudo-second-order model controlled adsorption process.

Conclusions

Nano-iron loaded mesoporous silica (FeO@mSiO2) nanocomposite was synthesised and study its characterization using FTIR, XRD, SEM, and TG analysis to Interpretation of the structure of matter of the synthesised material.$FeO@mSiO_2$ was proven to be capable of a good removal efficiency for Ni (II) and Co (II) at various condition. Under several usual pH conditions, the removal efficacy always remainder above 80%. The optimal sorption or removal occurred after a contact time ranging from 90 to120 minutes. The experimental data of the adsorption process under isothermal circumstances were analyzed. At varying temperatures, (FeO@mSiO2) demonstrated a removal effectiveness of almost 99.999% and 92.55% for Ni (II) and Co (II), respectively. Nanocomposite produced which can be synthesized using easily accessible equipment and at a cheap expense, offers a favourable choice for water treatment especially the heavy metals. Future work should thus include (a) optimization of the FeO-mSiO2 synthesis; (b) studies on the regeneration and re-usability of the composite and that of FeO-mSiO2; and (c) Study of the thermodynamic and mechanism properties of adsorption process.

CRediT authorship contribution statement

Wahran M. Saod: . **Nisreen Jassam Alaallah:** Validation, Data curation. **Ekhlas A. Abdulkareem:** Methodology. **Nahla Naji Hilal:** Writing – review & editing. **Mohammad I. AlBiajawi:** Writing – review & editing.

Declaration of competing interest

The authors declare that they have no known competing financial interests or personal relationships that could have appeared to influence the work reported in this paper.

Data availability

No data was used for the research described in the article.

References

[1] Q. Zhou, et al., Total concentrations and sources of heavy metal pollution in global river and lake water bodies from 1972 to 2017, Global Ecol. Conserv. 22 (2020).
[2] W.M. Saod, I.W. Oliver, D.F. Thompson, S. Holborn, A. Contini, V. Zholobenko, Magnesium oxide loaded mesoporous silica: Synthesis, characterisation and use in removing lead and cadmium from water supplies, Environ. Nanotechnol. Monit. Manage. 20 (2023).

[3] L.P. Lingamdinne, J.R. Koduru, H. Roh, Y.-L. Choi, Y.-Y. Chang, J.-K. Yang, Adsorption removal of Co (II) from waste-water using graphene oxide, Hydrometall. 165 (2016) 90–96.

[4] A. Babapoor, O. Rafiei, Y. Mousavi, M.M. Azizi, M. Paar, A. Nuri, Comparison and optimization of operational parameters in removal of heavy metal ions from aqueous solutions by low-cost adsorbents, Int. J. Chem. Eng. 2022 (2022) 1–21.

[5] Z.A. Alothman, Y.E. Unsal, M. Habila, M. Tuzen, M. Soylak, A membrane filtration procedure for the enrichment, separation, and flame atomic absorption spectrometric determinations of some metals in water, hair, urine, and fish samples, Desalin. Water Treat. 53 (13) (2015) 3457–3465.

[6] E.S. Agudosi, et al., Pilot study of in-line continuous flocculation water treatment plant, J. Environ. Chem. Eng. 6 (6) (2018) 7185–7191.

[7] M.C. Benalia, L. Youcef, M.G. Bouaziz, S. Achour, H. Menasra, Removal of heavy metals from industrial wastewater by chemical precipitation: mechanisms and sludge characterization, Arab. J. Sci. Eng. 47 (5) (2022) 5587–5599.

[8] L.K. Wang, Humanitarian engineering education of the Lenox Institute of Water Technology and its new potable water flotation processes, Environ. Flotat. Eng., Springer (2021) 1–72.

[9] M. Meena, P. Sonigra, G. Yadav, and T. Barupal, "Wastewater treatment techniques: An introduction," *Removal of emerging contaminants through microbial processes*, pp. 161–182, 2021.

[10] B.S. Thaçi, S.T. Gashi, Reverse osmosis removal of heavy metals from wastewater effluents using biowaste materials pretreatment, Pol. J. Environ. Stud. 28 (1) (2019) 337–341.

[11] G. Crini, E. Lichtfouse, Advantages and disadvantages of techniques used for wastewater treatment, Environ. Chem. Lett. 17 (2019) 145–155.

[12] R. Wagdy, M.F. Mubarak, R.S. Mohamed, A. El Shahawy, Industrial-scale feasibility for textile wastewater treatment via Photocatalysis-adsorption technology using black sand and UV lamp, RSC Adv. 14 (15) (2024) 10776–10789.

[13] H. Yin, B. He, H. Peng, J. Ye, F. Yang, N. Zhang, Removal of Cr (VI) and Ni (II) from aqueous solution by fused yeast: Study of cations release and biosorption mechanism, J. Hazard. Mater. 158 (2–3) (2008) 568–576.

[14] S. M. Mousavi *et al.*, "Separation of Ni (II) from Industrial Wastewater by Kombucha Scoby as a Colony Consisted from Bacteria and Yeast: Kinetic and Equilibrium Studies.," *Acta Chimica Slovenica*, vol. 66, no. 4, 2019.

[15] M.A. Hashem, Adsorption of lead ions from aqueous solution by okra wastes, Int. J. Phys. Sci. 2 (7) (2007) 178–184.

[16] A.M. Zayed, et al., Efficient dye removal from industrial wastewater using sustainable activated carbon and its polyamide nanocomposite derived from agricultural and industrial wastes in column systems, RSC Adv. 13 (36) (2023) 24887–24898.

[17] M. Kobya, E. Demirbas, E. Senturk, M. Ince, Adsorption of heavy metal ions from aqueous solutions by activated carbon prepared from apricot stone, Bioresour. Technol. 96 (13) (2005) 1518–1521.

[18] S.M. Mousavi, et al., Pb (II) removal from synthetic wastewater using Kombucha Scoby and graphene oxide/Fe3O4, Phys. Chem. Res. 6 (4) (2018) 759–771.

[19] S. M. Mousavi *et al.*, "Erythrosine Adsorption from Aqueous Solution via Decorated Graphene Oxide with Magnetic Iron Oxide Nano Particles: Kinetic and Equilibrium Studies.," *Acta Chimica Slovenica*, vol. 65, no. 4, 2018.

[20] W.M. Saod, I.W. Oliver, D.F. Thompson, A. Contini, V. Zholobenko, Zinc oxide–mesoporous silica nanocomposite: preparation, characterisation and application in water treatment for lead, cadmium and chromium removal, Int. J. Environ. Anal. Chem. 00 (00) (2023) 1–13, https://doi.org/10.1080/03067319.2023.2246016.

[21] W.M. Saod, I.W. Oliver, A. Contini, V. Zholobenko, Synthesis and characterisation of an iron oxide mesoporous silica nano-composite and its application in removal of methylene blue dye, J. Mol. Struct. 1319 (P1) (2025), https://doi.org/10.1016/j.molstruc.2024.139390.

[22] M.A. Tahoon, S.M. Siddeeg, N. Salem Alsaiari, W. Mnif, F. Ben Rebah, Effective heavy metals removal from water using nanomaterials: A review, Processes 8 (6) (2020) 645.

[23] J. Hong, J. Xie, S. Mirshahghassemi, J. Lead, Metal (Cd, Cr, Ni, Pb) removal from environmentally relevant waters using polyvinylpyrrolidone-coated magnetite nanoparticles, RSC Adv. 10 (6) (2020) 3266–3276.

[24] J. Jeevanandam, A. Barhoum, Y.S. Chan, A. Dufresne, M.K. Danquah, Review on nanoparticles and nanostructured materials: history, sources, toxicity and regulations, Beilstein J. Nanotechnol. 9 (1) (2018) 1050–1074.

[25] H.K. Hami, R.F. Abbas, E.M. Eltayef, N.I. Mahdi, Applications of aluminum oxide and nano aluminum oxide as adsorbents: review: Array, Samarra J. Pure Appl. Sci. 2 (2) (2020) 19–32.

[26] L. Khezamia, K.K. Tahaa, E. Amamic, I. Ghiloufid, L. El Mird, Removal of cadmium (II) from aqueous solution by zinc oxide nanoparticles: kinetic and thermodynamic studies, Desalin. Water Treat. 62 (2017) 346–354.

[27] S.H. Khan, B. Pathak, M.H. Fulekar, Nanomaterial for photocatalysis and their applications in environmental clean-up, Int. J. Curr. Res 7 (2015) 20850–20865.

[28] V.K. Yadav, M.H. Fulekar, Biogenic synthesis of maghemite nanoparticles (γ-Fe2O3) using Tridax leaf extract and its application for removal of fly ash heavy metals (Pb, Cd), Mater. Today Proc. 5 (9) (2018) 20704–20710.

[29] V.K. Yadav, et al., Microbial synthesis of nanoparticles and their applications for wastewater treatment, Microbial Biotechnol.: Basic Res. Appl. (2020) 147–187.

[30] M. Anjum, R. Miandad, M. Waqas, F. Gehany, M.A. Barakat, Remediation of wastewater using various nano-materials, Arab. J. Chem. 12 (8) (2019) 4897–4919.

[31] V. Mulens-Arias, J.M. Rojas, D.F. Barber, The intrinsic biological identities of iron oxide nanoparticles and their coatings: Unexplored territory for combinatorial therapies, Nanomaterials 10 (5) (2020) 837.

[32] F. Fu, D.D. Dionysiou, H. Liu, The use of zero-valent iron for groundwater remediation and wastewater treatment: a review, J. Hazard. Mater. 267 (2014) 194–205.

[33] A. López-Ortega, M. Estrader, G. Salazar-Alvarez, A.G. Roca, J. Nogués, Applications of exchange coupled bi-magnetic hard / soft and, Phys. Rep. 553 (2014) 1–32, https://doi.org/10.1016/j.physrep.2014.09.007.1.

[34] Y. Song, S. Chen, Janus nanoparticles: Preparation, characterization, and applications, Chem. Asian J. 9 (2) (2014) 418–430, https://doi.org/10.1002/asia.201301398.

[35] S. Talebzadeh, C. Queffélec, D.A. Knight, Surface modification of plasmonic noble metal-metal oxide core-shell nanoparticles, Nanoscale Adv. 1 (12) (2019) 4578–4591, https://doi.org/10.1039/c9na00581a.

[36] N. Safaie and R. C. Ferrier, "Janus nanoparticle synthesis: Overview, recent developments, and applications," *J. Appl. Phys.*, vol. 127, no. 17, 2020, doi: 10.1063/5.0003329.

[37] E. Fantechi, et al., Seeded Growth Synthesis of Au-Fe3O4 Heterostructured Nanocrystals: Rational Design and Mechanistic Insights, Chem. Mater. 29 (9) (2017) 4022–4035, https://doi.org/10.1021/acs.chemmater.7b00608.

[38] P.D. Cozzoli, T. Pellegrino, L. Manna, Synthesis, properties and perspectives of hybrid nanocrystal structures, Chem. Soc. Rev. 35 (11) (2006) 1195–1208, https://doi.org/10.1039/b517790c.

[39] T.C. Le, J. Zhai, W.H. Chiu, P.A. Tran, N. Tran, Janus particles: Recent advances in the biomedical applications, Int. J. Nanomed. 14 (2019) 6749–6777, https://doi.org/10.2147/IJN.S169030.

[40] A.C. Anselmo, S. Mitragotri, Nanoparticles in the clinic: An update, Bioeng. Transl. Med. 4 (3) (2019) 1–16, https://doi.org/10.1002/btm2.10143.

[41] D. Bobo, K.J. Robinson, J. Islam, K.J. Thurecht, S.R. Corrie, Nanoparticle-Based Medicines: A Review of FDA-Approved Materials and Clinical Trials to Date, Pharm. Res. 33 (10) (2016) 2373–2387, https://doi.org/10.1007/s11095-016-1958-5.

[42] A.C. Anselmo, S. Mitragotri, Nanoparticles in the clinic, Bioeng. Transl. Med. 1 (1) (2016) 10–29, https://doi.org/10.1002/btm2.10003.

[43] [43] I. A. Mawlood, W. M. Saod, A. S. Al-Rawi, A. M. Aljumialy, and N. Hilal, "Characterization and use of activated carbon synthesized from sunflower seed shell in the removal of Pb(II), Cd(II), and Cr(III) ions from aqueous solution," *Environmental Monitoring and Assessment*, vol. 196, no. 4, 2024, doi: 10.1007/s10661-024-12525-1.

[44] M. Sadia, M.R. Jan, J. Shah, G.M. Greenway, Simultaneous preconcentration and determination of nickel and cobalt using functionalised mesoporous silica spheres by ICP-OES, Int. J. Environ. Anal. Chem. 93 (14) (2013) 1537–1556, https://doi.org/10.1080/03067319.2013.823487.

[45] R. Chakraborty, A. Asthana, A.K. Singh, B. Jain, A.B.H. Susan, Adsorption of heavy metal ions by various low-cost adsorbents: a review, Int. J. Environ. Anal. Chem. 102 (2) (2022) 342–379, https://doi.org/10.1080/03067319.2020.1722811.

[46] A. Heidari, H. Younesi, Z. Mehraban, Removal of Ni(II), Cd(II), and Pb(II) from a ternary aqueous solution by amino functionalized mesoporous and nano mesoporous silica, Chem. Eng. J. 153 (1–3) (2009) 70–79, https://doi.org/10.1016/j.cej.2009.06.016.

[47] M. Anbia, K. Kargosha, S. Khoshbooei, Heavy metal ions removal from aqueous media by modified magnetic mesoporous silica MCM-48, Chem. Eng. Res. Des. 93 (2015) 779–788, https://doi.org/10.1016/j.cherd.2014.07.018.

[48] I.M. El-Nahhal, J.K. Salem, S. Kuhn, T. Hammad, R. Hempelmann, S. Al Bhaisi, Synthesis & characterization of silica coated and functionalized silica coated zinc oxide nanomaterials, Powder Technol. 287 (2016) 439–446.

[49] R. Chanda, A.H. Mithun, M.A. Hasan, B.K. Biswas, Nickel removal from aqueous solution using chemically treated mahogany sawdust as biosorbent, J. Chem. 2021 (2021) 1–10.

[50] Z.A. Alothman, et al., Low cost biosorbents from fungi for heavy metals removal from wastewater, Sep. Sci. Technol. 55 (10) (2020) 1766–1775.

[51] O.A. Adigun, V.O. Oninla, N.A.A. Babarinde, K.O. Oyedotun, N. Manyala, Characterization of sugarcane leaf-biomass and investigation of its efficiency in removing Nickel (II), Chromium (III) and Cobalt (II) ions from polluted water, Surf. Interfaces 20 (2020).

[52] E. Daneshvar, A. Vazirzadeh, A. Niazi, M. Sillanpää, A. Bhatnagar, A comparative study of methylene blue biosorption using different modified brown, red and green macroalgae–Effect of pretreatment, Chem. Eng. J. 307 (2017) 435–446.

[53] J. Long, X. Huang, X. Fan, Y. Peng, J. Xia, Effective adsorption of nickel (II) with Ulva lactuca dried biomass: isotherms, kinetics and mechanisms, Water Sci. Technol. 78 (1) (2018) 156–164.

[54] S. Ratan, I. Singh, J. Sarkar, R.M. Naik, The removal of nickel from waste water by modified coconut coir pith, Chem. Sci. J. 7 (3) (2016) 1–6.

[55] M. Rafatullah, O. Sulaiman, R. Hashim, A. Ahmad, Adsorption of copper (II), chromium (III), nickel (II) and lead (II) ions from aqueous solutions by meranti sawdust, J. Hazard. Mater. 170 (2–3) (2009) 969–977.

[56] M. Nigam, S. Rajoriya, S.R. Singh, P. Kumar, Adsorption of Cr (VI) ion from tannery wastewater on tea waste: kinetics, equilibrium and thermodynamics studies, J. Environ. Chem. Eng. 7 (3) (2019).

[57] P. N. Dave, N. Pandey, and H. Thomas, "Adsorption of Cr (VI) from aqueous solutions on tea waste and coconut husk," 2012.

[58] O.A. Oyewo, B. Mutesse, T.Y. Leswifi, M.S. Onyango, Highly efficient removal of nickel and cadmium from water using sawdust-derived cellulose nanocrystals, J. Environ. Chem. Eng. 7 (4) (2019).

[59] Y. Wu, H. Luo, H. Wang, L. Zhang, P. Liu, L. Feng, Fast adsorption of nickel ions by porous graphene oxide/sawdust composite and reuse for phenol degradation from aqueous solutions, J. Colloid Interface Sci. 436 (2014) 90–98.

[60] G. Enaime, A. Baçaoui, A. Yaacoubi, and M. Lübken, "Applsci-10-03492.Pdf," 2020.

[61] S. Lyubchik, A. Lyubchik, O. Lygina, S. Lyubchik, I. Fonsec, Comparison of the Thermodynamic Parameters Estimation for the Adsorption Process of the Metals from Liquid Phase on Activated Carbons, Thermodynamics - Interaction Studies - Solids Liquids and Gases (2011), https://doi.org/10.5772/19514.

[62] M. Changalvaei, M.R. Nilforoushan, A. Arabmarkadeh, M. Tayebi, Removal of Ni and Zn heavy metal ions from industrial waste waters using modified slag of electric arc furnace, Mater. Res. Express 8 (5) (2021) 55506.

[63] Š. Abdić, M. Memić, E. Šabanović, J. Sulejmanović, S. Begić, Adsorptive removal of eight heavy metals from aqueous solution by unmodified and modified agricultural waste: tangerine peel, Int. J. Environ. Sci. Technol. 15 (2018) 2511–2518.

[64] D.-H. Vu, et al., A novel approach in adsorption of heavy metal ions from aqueous solution using synthesized MCM-41 from coal bottom ash, Int. J. Environ. Anal. Chem. 100 (11) (2020) 1226–1244.

[65] C.P. Guthrie, E.J. Reardon, Metastability of MCM-41 and Al-MCM-41, Chem. A Eur. J. 112 (15) (2008) 3386–3390.

[66] A.M. Ahmed, R. Hosny, M.F. Mubarak, A.A. Younes, A.B. Farag, Green magnetic clay nanocomposite based on graphene oxide nanosheet as a synthetic low-cost adsorbent for oil droplets removal from produced water, Desalin. Water Treat. 280 (2022) 206–223.

[67] S. Jain, R.K. Vyas, P. Pandit, A.K. Dalai, Adsorption of antiviral drug, acyclovir from aqueous solution on powdered activated charcoal: kinetics, equilibrium, and thermodynamic studies, Desalin. Water Treat. 52 (25–27) (2014) 4953–4968.

[68] Z. B. Bouabidi, M. H. El-naas, D. Cortes, G. Mckay, D. Cortes, and G. Mckay, "Accepted Manuscript," no. Ii, 2017.

[69] S. Tamjidi, H. Esmaeili, and B. Kamyab Moghadas, "Application of magnetic adsorbents for removal of heavy metals from wastewater: A review study," *Mater. Res. Expr.*, vol. 6, no. 10, 2019, doi: 10.1088/2053-1591/ab3ffb.

[70] M. Abedpour, B. Kamyab Moghadas, S. Tamjidi, Equilibrium and kinetic study of simultaneous removal of Cd (II) and Ni (II) by acrylamide-based polymer as effective adsorbent: optimisation by response surface methodology (RSM), Int. J. Environ. Anal. Chem. 102 (15) (2022) 3524–3541, https://doi.org/10.1080/03067319.2020.1772768.